High purity β-Bi$_2$O$_3$ preparation by thermal decomposition of tartrates

Evgeniya V. Timakova [ab] * , Tatiana E. Timakova [ab] , Liubov I. Afonina [ab]

a: Department of Chemistry and Chemical Technology, Novosibirsk State Technical University, Novosibirsk 630073, Russia

b: Institute of Solid State Chemistry and Mechanochemistry, Siberian Branch of the RAS, Novosibirsk 630090, Russia

* Corresponding author: timakova@solid.nsc.ru

Abstract

The processes of oxidative thermolysis of bismuth(III) DL-tartrate BiC$_4$H$_3$O$_6$ obtained by the interaction of high-purity basic bismuth(III) nitrates [Bi$_6$O$_4$(OH)$_4$](NO$_3$)$_6$·H$_2$O and [Bi$_6$O$_5$(OH)$_3$](NO$_3$)$_5$·3H$_2$O with DL-tartaric acid solution have been investigated. The products of precipitation have been studied by methods of X-ray diffraction and thermal analysis, IR and Raman spectroscopy and chemical analysis. The staging of thermal transformation processes has been determined. Morphological studies and grain size analysis of initial precursors and final products of their thermal transformations have been carried out. The possibility of obtaining fine crystalline powders of tetragonal bismuth(III) oxide modification β-Bi$_2$O$_3$ by oxidative thermolysis of DL-BiC$_4$H$_3$O$_6$ has been shown.

Key finding

● Fine crystalline powders of high purity tetragonal bismuth(III) oxide β-Bi$_2$O$_3$ were obtained from the decomposition of the precursor DL-BiC$_4$H$_3$O$_6$ synthesized from basic bismuth(III) nitrates.

1. Introduction

Tartrates are widely used as precursors for the preparation of fine crystalline and nanodispersed powders of metals, their oxides [1–4] and mixed oxide materials [5–8] by thermolysis in inert and oxidizing atmospheres. Bismuth tartrate precursors are also used to produce bismuth oxides [9] and bismuth-based materials [10, 11]. We have investigated the thermal decomposition of bismuth tartrate [Bi(NO$_3$)(C$_4$H$_4$O$_6$)]·3H$_2$O obtained by adding a bismuth solution in nitric acid to a solution of L(+)-tartaric acid [12]. It has been shown that thermolysis of [Bi(NO$_3$)(C$_4$H$_4$O$_6$)]·3H$_2$O in air atmosphere for 6 h at 300 °C with preliminary holding at lower temperatures produces a mixture of tetragonal bismuth(III) oxide and bismuth(III) oxocarbonate β-Bi$_2$O$_3$/(BiO)$_2$CO$_3$. With increasing temperature, a β→α phase transition occurs and the final decomposition product is the monocline modification, α-Bi$_2$O$_3$. Monophase fine crystalline powders of tetragonal bismuth oxide β-Bi$_2$O$_3$ were obtained by oxidative thermolysis of bismuth(III) tartrate BiC$_4$H$_3$O$_6$·H$_2$O for 6 h at 280 °C. BiC$_4$H$_3$O$_6$·H$_2$O is an X-ray amorphous compound obtained by multiple washing of [Bi(NO$_3$)(C$_4$H$_4$O$_6$)]·3H$_2$O with water. Direct precipitation of BiC$_4$H$_3$O$_6$·H$_2$O from nitric acid solutions does not provide effective purification from nitrate ions, and obtaining this compound by multiple washings with water [Bi(NO$_3$)(C$_4$H$_4$O$_6$)]·3H$_2$O is a lengthy process. Therefore, it is of interest to consider the process of obtaining BiC$_4$H$_3$O$_6$·H$_2$O by treating solid bismuth precursors with tartaric acid solution.

It is reasonable to consider basic bismuth(III) nitrates as precursors for obtaining bismuth tartrate. It has been shown [13] that bismuth precipitation in the form of basic nitrates, during the hydrolytic processing of technological nitric acid solutions prepared from metallic bismuth of Bi1 grade and containing impurities of accompanying metals, allows high values of bismuth purification coefficients from impurities to be achieved. Hydrolysis at elevated temperatures not lower than 60 °C allows obtaining easily filterable precipitate of the composition [Bi$_6$O$_4$(OH)$_4$](NO$_3$)$_6$·H$_2$O (further basic bismuth(III) nitrate) and separating it effectively from the mother liquor containing impurity metal ions. Washing this compound

with water results in hydrolytic decomposition to form the $[Bi_6O_5(OH)_3](NO_3)_5 \cdot 3H_2O$. As a result of recrystallization, the final product is effectively purified from metal impurities captured in the volume of microcrystals during the precipitation of the primary hydrolysis product. The use of $[Bi_6O_4(OH)_4](NO_3)_6 \cdot H_2O$ and $[Bi_6O_5(OH)_3](NO_3)_5 \cdot 3H_2O$ as precursors for further treatment with carboxylic acids or alkaline reagents makes this process widely applicable for the synthesis of high-purity bismuth compounds for engineering and medicine.

The aim of this work was the synthesis of high purity bismuth(III) tartrate by the reaction "basic bismuth(III) nitrates – tartaric acid solution" followed by the production of tetragonal β-Bi_2O_3.

2. Experimental

All reagents (acids, bases and salts) in this work were of analytical grade and were used without further purification.

Metallic bismuth Bi1 (Kazzinc, GOST (State Standard) 10928–90) was used. The metal contents were (wt.%): 99.1 bismuth, 0.71 lead, $1.0 \cdot 10^{-3}$ zinc, $1.0 \cdot 10^{-3}$ antimony, $3.3 \cdot 10^{-3}$ copper, $1.0 \cdot 10^{-1}$ silver, $2.0 \cdot 10^{-4}$ arsenic, $1.0 \cdot 10^{-3}$ iron and $1.0 \cdot 10^{-4}$ tellurium.

Bismuth stock solution in nitric acid (420 g·l⁻¹ bismuth and 100 g·l⁻¹ free HNO_3) was prepared by dissolving technical bismuth oxide, obtained according to ref. [14], in nitric acid with the concentration of 7 mol·l⁻¹. The hydrolytic precipitation of bismuth from nitric acid solution, as well as investigation of "solid precursor – carboxylic acid solution" processes were carried out in fluoroplastic or glass vessels equipped with stirrers and thermostatically controlled in water baths.

Hydrate tetrahydroxo-tetraoxo-hexabismuth(III) hexanitrate of $[Bi_6O_4(OH)_4](NO_3)_6 \cdot H_2O$ was prepared by adding 50 ml of distilled water heated to 55–60 °C to 50 ml of bismuth nitrate solution with stirring, then 36 ml of ammonium carbonate solution with a concentration of 2.5 mol·l⁻¹ to pH = 1. The mixture was stirred for 30 min and allowed to stand for 1 h. The mother liquor was separated from the sediment by decantation, the sediment was washed with 150 ml of nitric acid solution with a concentration of 0.1 mol·l⁻¹ for 30 min at 60 °C. Trihydrate trihydroxo-pentaoxo-hexabismuth(III) pentanitrate of the composition $[Bi_6O_5(OH)_3](NO_3)_5 \cdot 3H_2O$ was obtained by washing the precipitate twice with 150 ml of distilled water for 30 min at 60 °C.

For the synthesis of bismuth(III) tartrate 10 g of freshly prepared basic bismuth(III) nitrates $[Bi_6O_4(OH)_4](NO_3)_6 \cdot H_2O$ or $[Bi_6O_5(OH)_3](NO_3)_5 \cdot 3H_2O$ was stirred for 10 min in 90 ml distilled water to the resulting mixture was added the required amount of tartaric acid $C_4H_6O_6$. The molar ratio of tartrate ions to bismuth was 1.1. The resulting mixture was stirred for 1–2 h at 70 °C. The resulting precipitate was filtered off, washed 2 times with distilled water at the synthesis temperature and dried in air.

Bismuth(III) oxocarbonate of the composition $(BiO)_2CO_3$ was obtained by treating $[Bi_6O_4(OH)_4](NO_3)_6 \cdot H_2O$ or $[Bi_6O_5(OH)_3](NO_3)_5 \cdot 3H_2O$ with ammonium carbonate solution at pH ≥ 8 and 25 °C [13].

Chemical determination of macro quantities of Bi(III) in solutions was carried out by titration with complexon III solution in the presence of xylenol orange indicator. Micro quantities of Bi(III) were determined by photocolorimetric method using potassium iodide. Carbon, nitrogen and hydrogen contents in the obtained samples were determined by modified Pregle method with gravimetric termination.

The phase compositions of the samples were analyzed using X-ray diffraction technique (XRD) on a diffractometer (Bruker D8 Advance, Germany) using Cu Kα radiation (λ = 1.5418 Å). X-ray diffraction data were collected in scanning mode at a scanning speed of 0.5°·min⁻¹ in the range of 4° < 2θ < 70°. Phase analysis was performed using the ICDD PDF-4 database (2011).

The IR absorption spectra in the range 400–4000 cm⁻¹ were recorded with a IR-Fourier spectrometer Tensor 27 (Bruker, Germany). The samples were prepared as tablets with calcined KBr. Raman spectra were taken on a T64000 spectrometer (Horiba Jobin Yvon, Japan) with an Ar⁺ laser (wavelength 514.5 nm, Z(XY)-Z geometry). Microstructure of the samples was studied by scanning electron microscopy (SEM) using a Hitachi TM 1000 Scanning Electron Microscope.

Thermal analysis of the samples was carried out on a synchronous thermoanalytical complex STA 449 F1 Jupiter (Netzsch) dynamically under heating in an Ar/O₂ atmosphere (80/20; O₂ 10 ml·min⁻¹; Ar 40 ml·min⁻¹). Samples weighing 20–50 mg were placed in crucibles of Pt – 10% Rh alloy and heated at a rate of 10 deg·min⁻¹ to 350–500 °C. The mass spectra of the gaseous products formed in the course of the heat treatment were recorded in the multi-ion detection mode at m/z of 18 and 44 with a QMS 403D quadrupole mass spectrometer (Netzsch).

Particle size analysis of powders was performed using a laser particle size analyzer Microsizer 201A (VA Instalt, Russia).

3. Results and Discussion

3.1. Synthesis and characterization of bismuth DL-tartrate

According to the XRD analysis, the treatment of freshly precipitated $[Bi_6O_4(OH)_4](NO_3)_6 \cdot H_2O$ (Figure 1, curve 1) with a solution of L(+)-tartaric acid at a molar ratio of $n(C_4H_4O_6^{2-}/Bi^{3+}) = 1.1$ at 70 °C within 1 h leads to the formation of a mixture of $[Bi_6O_4(OH)_4](NO_3)_6 \cdot H_2O$ [13] and $[Bi_6O_5(OH)_3](NO_3)_5 \cdot 3H_2O$ (ICDD 000-48-0575) (Figure 1, curve 2). Increasing the exposure time to 2 h gives $[Bi_6O_5(OH)_3](NO_3)_5 \cdot 3H_2O$ (Figure 1, curve 3). When $[Bi_6O_5(OH)_3](NO_3)_5 \cdot 3H_2O$ is treated with L(+)-tartaric acid solution, the initial precursor remains as a synthesis product. Thus, in the system "basic bismuth(III) nitrates -

solution of L(+)-tartaric acid" under the chosen conditions, bismuth tartrate is not formed.

Considering the possibility of using the racemic form of tartaric acid for the synthesis of tartrate precursors [15–17], we chose DL-tartaric acid to obtain bismuth tartrate.

According to the XRD data, the treatment of basic bismuth(III) nitrates with DL-tartaric acid solution at $n = 1.1$ and temperature 70 °C for 1–2 h leads to the formation of bismuth tartrate of a $BiC_4H_3O_6$ composition (Figure 1, curve 4), which is confirmed by the data of chemical analysis, content in %: Bi – 60.1 (theor. 58.7); C – 12.7 (13.5) and H – 0.75 (0.84). $DL-BiC_4H_3O_6$ has a low degree of crystallinity: an intense reflex is observed on the diffractogram of the compound at $d/n = 6.57$ Å ($2\theta = 13.46°$), other reflexes are broadened and have low intensity.

The analysis of IR and Raman spectra of DL-tartaric acid and its bismuth salt allowed us to conclude the form of the presence of tartaric acid residues in $DL-BiC_4H_3O_6$ and the way of their connection with metal atoms. The assignment of vibrational bands in the IR and Raman spectra of $DL-BiC_4H_3O_6$ was carried out in comparison with the spectra of DL-tartaric acid based on literature data [18, 19].

Tartaric acid can form complex compounds with metals due to carboxylic and alcohol (oxy) groups, so it is necessary to analyze the characteristic vibrational bands of these functional groups. Calculations of the vibrational spectrum of tartaric acid [18] showed that only the stretching vibrations of OH, CH, and C=O groups are specific in shape and wavenumbers, while the other vibrations are strongly mixed. Therefore, let us consider in detail the changes observed in the spectrum of the salt as compared to the spectrum of the acid.

In the spectra of DL-tartaric acid (Figures 2 and 3, curve 1) the presence of OH-groups involved in the formation of intermolecular hydrogen bonding is indicated by a broad band in the range of 3650–3280 cm⁻¹, divided into two components at 3413 (IR), 3408 (Raman) and 3365 (IR), 3354 (Raman), assigned to the stretching vibrations of ν(O–H) alcohol and carboxyl groups, respectively [18]. Stretching vibrations of the C=O bond of dimeric carboxyl groups linked by intermolecular hydrogen bonds correspond to a strong band at 1743 (IR), 1690 (Raman) cm⁻¹ and those involved in intramolecular hydrogen bonds at 1635 (IR), 1653 (Raman) cm⁻¹. These bands are not recorded in the spectrum of bismuth salt (Figures 2 and 3, curve 2). In the above spectra bands related to asymmetric $\nu_{as}(COO^-)$ and symmetric $\nu_s(COO^-)$ stretching vibrations of ionized COO^- groups at (cm⁻¹): 1595, 1555 (IR); 1583, 1558 (Raman) and 1404, 1362 (IR); 1404, 1363 (Raman) respectively are present, which denotes substitution of protons in the carboxyl groups of carboxylic acid by Bi-containing cation. Presence of several asymmetric and symmetric bands of carboxylate ions indicates different structural functions performed by them. The broad band in the range of 3650-3300 cm⁻¹ in the IR spectrum refers to alcohol groups not substituted by bismuth cation and involved in intermolecular hydrogen bonds.

In the range of 1460-1200 cm⁻¹ several bands of in-plane bending vibration β(OH) overlapping with in-plane bending β(C–H) are observed in acid spectra (Figures 2 and 3, curve 1): the medium and strong bands 1455, 1401 (IR) and 1457, 1391 (Raman) refer to in-plane bending vibration of alcohol groups, and weak bands 1327 (IR), 1330 (Raman) to carboxyl groups [18].

In the spectra of the acid (Figures 2 and 3, curve 1), the bands of stretching vibrations ν(C–H) at 2971, 2912 (IR) and 2972, 2923 (Raman) cm⁻¹ are observed. In the spectra of the salt (Figures 2 and 3, curve 2) these vibrations correspond to bands at 1289, 1258 (IR) and 1283, 1263 (Raman) cm⁻¹.

In the IR spectrum of the acid a series of strong and medium bands belonging to in-plane bending vibrations of β(C–C–H) at 1291, 1257, 1238, 1220 cm⁻¹ (Figure 2, curve 1) are observed. In the Raman spectrum these bands are observed at wavenumbers of 1263, 1245, 1219 cm⁻¹ (Figure 3, curve 1), these vibrations also overlap with in-plane bending vibrations of hydroxyl groups [18]. When the protons of OH-groups are substituted by bismuth cation, the disappearance of several bands, decrease of intensity and broadening of bands registered at 1289, 1258 (IR) and 1283, 1263 (Raman) cm⁻¹ are observed in the spectra of salt (Figures 2 and 3, curve 2).
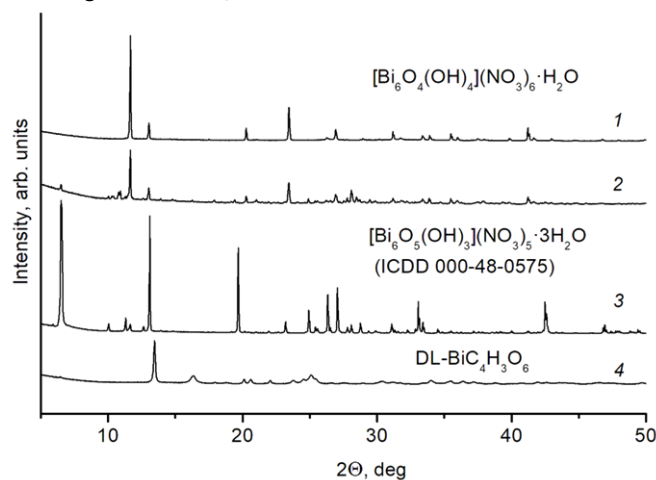
Figure 1 X-ray powder diffraction patterns of the initial $[Bi_6O_4(OH)_4](NO_3)_6 \cdot H_2O$ (1) and treated by L(+)- (2, 3) and DL- (4) $C_4H_6O_6$. Synthesis conditions: 70 °C, $n = 1.1$, 1 h (2, 4), 2 h (3).
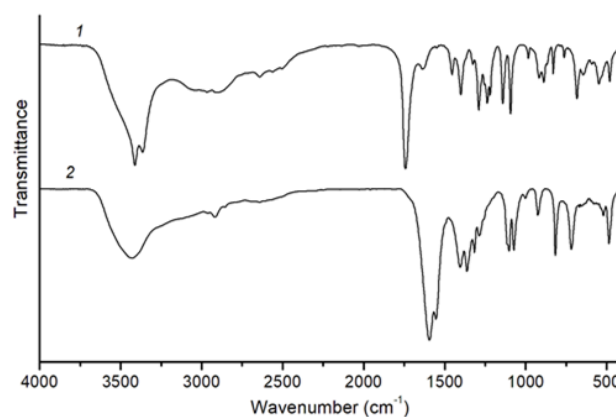
Figure 2 IR spectra of $DL-C_4H_6O_6$ (1) and $DL-BiC_4H_3O_6$ (2).

In the acid spectrum strong bands at 1142 (IR) and 1151 (Raman) cm^{-1} related to the stretching vibrations of ν(C–O) carboxyl groups are observed. For alcohol groups, these vibrations appear as a strong band in the IR spectrum at 1095 cm^{-1} and a weak band in the Raman spectrum at 1089 cm^{-1} [18]. At replacement of protons of carboxylic and alcohol groups by bismuth cation, these bands in bismuth salt spectra (Figures 2 and 3, curve 2) shift to the region of lower wavenumbers and additionally the third band appears, which is connected with C–O–Bi bond formation and participation of oxygen of non-dissociated alcohol group in bismuth cation coordination.

In the region of 1150-850 cm^{-1}, the stretching vibrations ν(C–C) are recorded as bands of medium intensity at 984, 918, 889, 868, 831 (IR) and 991, 900, 889, 873, 833 (Raman) cm^{-1} (Figures 2 and 3, curve 1). These bands are mixed with stretching and deformation vibrations of C–O bonds [18]. Therefore, changes are also observed in this region in the salt spectrum, consisting in a decrease in the number of vibration bands and a change in their intensity. Thus, in the IR spectrum of salt (Figure 2, curve 2) bands are observed: weak at 1003 cm^{-1} and medium at 925 cm^{-1}; in the Raman spectra (Figure 3, curve 2) these vibrations appear as medium and weak bands at 1006 and 925 cm^{-1} respectively. Out-of-plane bending vibrations δ(C–C=O) include bands at 831–482 cm^{-1} in the spectra of acid (Figures 2 and 3, curve 1) [18]. These bands are not registered in the salt spectra. The strong band at 818 cm^{-1} (Figure 2, curve 2) in the IR spectrum of salt and weak bands at 827, 817 cm^{-1} in the Raman spectrum (Figure 3, curve 2) are related to scissor vibrations of the carboxylate ion δ_s(COO$^-$) [19]. The presence of two δ_s(COO$^-$) bands in the Raman spectrum confirms the different structural functions of carboxylate ions. A strong band in the IR spectrum of the salt at 719 cm^{-1} refers to the torsional vibrations of δ_τ(COO$^-$) [20]. Stretching vibrations ν(Bi–O) include an intense band at 486 cm^{-1} with the shoulder at 476 cm^{-1} [21] in the infrared spectrum of the salt (Figure 2, curve 2). These vibrations are recorded in the Raman spectrum (Figure 3, curve 2) as a strong band with two maxima at 483 and 475 cm^{-1}, which indicate the unequal formation of metal-oxygen bonds. The absence of in-plane bending vibrations β(OH) bands of water molecules at 1630–1600 cm^{-1} indicates the formation of anhydrous salt [22].

Thus, the proposed composition of $BiC_4H_3O_6$ for bismuth DL-tartrate is in agreement with the physicochemical studies carried out and also confirmed by IR and Raman spectroscopy.

3.2. Thermal analysis of bismuth DL-tartrate

Thermal analysis data in Ar/O_2 atmosphere also confirm the composition of the synthesized compound (Figure 4): it is stable up to 220 ºC and does not contain crystallization water. This fact indicates the possibility of drying DL-$BiC_4H_3O_6$ samples at a temperature of 100–150 ºC during their industrial preparation and the possibility of long-

term storage at room temperature. Further thermolysis of DL-$BiC_4H_3O_6$ samples proceeds with exothermic effect in the temperature range 230–280 ºC. Its maximum observed around 275 ºC is related to tartrate ions decomposition/oxidation; according to mass spectrometry, it is accompanied by water and carbon dioxide removal.

The minimum on the TG curve at 265 ºC indicates the formation of metallic bismuth as a result of its reduction by carbon of tartrate ions, a further increase in mass is associated with the oxidation of metallic bismuth to oxide. In parallel, the decomposition of bismuth(III) oxocarbonate resulting from the thermolysis of bismuth tartrate also proceeds. According to mass spectrometry, these processes are accompanied by the release of carbon dioxide. Thus, the process of oxidative thermolysis of DL-$BiC_4H_3O_6$ is rather complicated and the effects on the DSC curve at temperature $\geq$345 ºC corresponding to the phase transition of tetragonal modification β-Bi_2O_3 into monocline α-Bi_2O_3 [23], indicate only a mixture of α- and β-Bi_2O_3 as a result of non-isothermal linear heating of the sample. The total mass loss of salt decomposition to Bi_2O_3 is 34.5% and agrees with the theoretical value (34.55%).
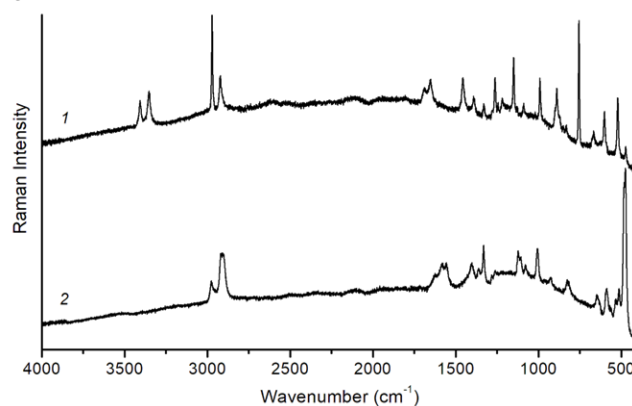

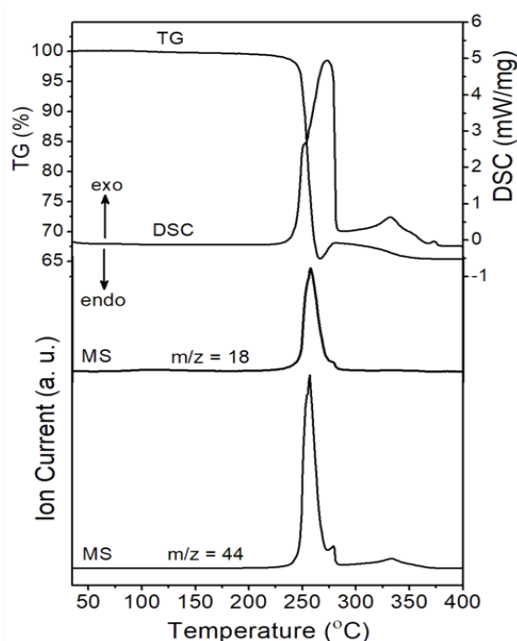**Figure 3** Raman spectra of DL-$C_4H_6O_6$ (1) and DL-$BiC_4H_3O_6$ (2).

Figure 4 The TG-DSC curves of DL-$BiC_4H_3O_6$ and MS signals of H_2O and CO_2.

According to XRD data (Figure 5, curve 1), the samples DL-BiC$_4$H$_3$O$_6$ aged in air at 280 ºC for 6 h represent a mixture of α-, β-Bi$_2$O$_3$ and metallic bismuth. A decrease of annealing temperature to 240–270 ºC also leads to the formation of the specified mixture of substances. The DL-BiC$_4$H$_3$O$_6$ samples were successively keeping at temperatures of 200, 220 and 240 ºC. According to XRD data, holding the sample at 200 ºC for 3 h does not lead to significant changes. Its diffractogram (Figure 5, curve 2) coincides with the initial one for DL-BiC$_4$H$_3$O$_6$ (Figure 1, curve 4). Further heating of sample at 220 ºC for 3–6 h leads to its amorphization (Figure 5, curve 3).

In the infrared spectrum of this sample, the vibrational bands of DL-BiC$_4$H$_3$O$_6$ (Figure 6, curves 1 and 2) are not observed. At the same time, the bands typical for bismuth(III) oxocarbonate of (BiO)$_2$CO$_3$ composition appear (Figure 6, curve 3). Thus, we can assume the formation of X-ray amorphous (BiO)$_2$CO$_3$ during keeping of DL-BiC$_4$H$_3$O$_6$ at 220 ºC. This assumption is confirmed by further exposure of the sample at 240 ºC. On the diffractogram of this sample (Figure 5, curve 4) the (BiO)$_2$CO$_3$ (ICDD 000-41-1488) reflexes are observed at the background of X-ray amorphous halo. On the basis of the studies carried out, the following scheme can be proposed for obtaining β-Bi$_2$O$_3$. The samples of DL-BiC$_4$H$_3$O$_6$ are successively kept at 220 ºC for 3–6 h and then at 280 ºC for 3–6 h. As a result, the single-phase samples of β-Bi$_2$O$_3$ are obtained (ICDD 010-77-5341, Figure 5, curve 5).

According to SEM data, [Bi$_6$O$_4$(OH)$_4$](NO$_3$)$_6$·H$_2$O precipitated from nitric acid solutions by ammonium carbonate is well formed short prismatic crystals with the largest single crystal size in the basic plane of 3–10 μm and 1–3 μm thick (Figure 7a).

As a result of washing [Bi$_6$O$_4$(OH)$_4$](NO$_3$)$_6$·H$_2$O with water, the obtained [Bi$_6$O$_5$(OH)$_3$](NO$_3$)$_5$·3H$_2$O, is an elongated prismatic crystal with a length in the basic plane of 4–20 μm, width of 2–8 μm and thickness of 1–3 μm (Figure 7b). In the subsequent step of the treatment of freshly prepared basic bismuth(III) nitrates with DL-tartaric acid solution, the resulting DL-BiC$_4$H$_3$O$_6$ samples are aggregates of 5–30 μm, consisting of needle-like particles of 1-3 μm length and 0.1–0.3 μm thickness, both synthesized from [Bi$_6$O$_4$(OH)$_4$](NO$_3$)$_6$·H$_2$O (Figure 7c) and from [Bi$_6$O$_5$(OH)$_3$](NO$_3$)$_5$·3H$_2$O (Figure 7d). The β-Bi$_2$O$_3$ samples obtained by oxidative thermolysis inherit the morphology of DL-BiC$_4$H$_3$O$_6$, also presenting aggregates of different sizes (Figure 7e, f).

For the synthesized powders DL-BiC$_4$H$_3$O$_6$ and the β-Bi$_2$O$_3$ samples obtained from them, their particle size distribution was analyzed, the results of which are shown in Figure 8.

Table 1 shows the values of average particle/aggregate size (D_l), the values of their standard deviations (σ), the degree of asymmetry of particle distribution (S_k) calculated by "geometric" method [24] and the value of 50 wt.% particle/aggregate size (D_{50}).
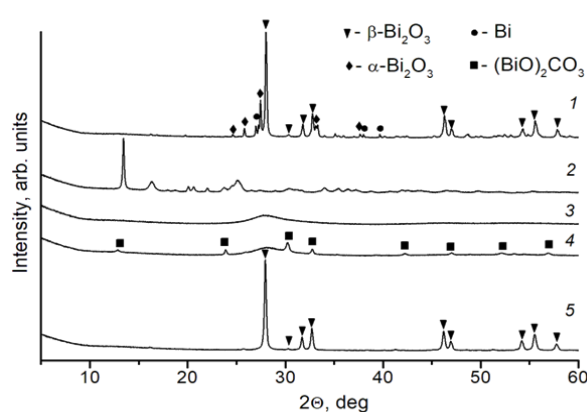

Figure 5 X-ray powder diffraction patterns of DL-BiC$_4$H$_3$O$_6$ samples aged at different temperatures. Exposure temperature: 280 (1), 200 (2), 220 (3), 240 (4), 220 and then 280 ºC (5). Curing times: 6 h (1), 3 h (2–4), 6 h (5).
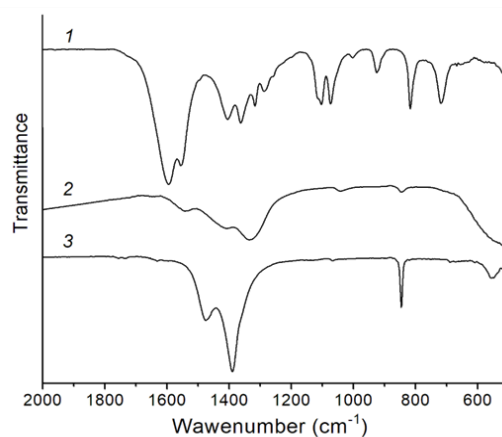
Figure 6 IR spectra of DL-BiC$_4$H$_3$O$_6$ (1), DL-BiC$_4$H$_3$O$_6$ incubated at 220 ºC for 6 h (2) and (BiO)$_2$CO$_3$ (3).
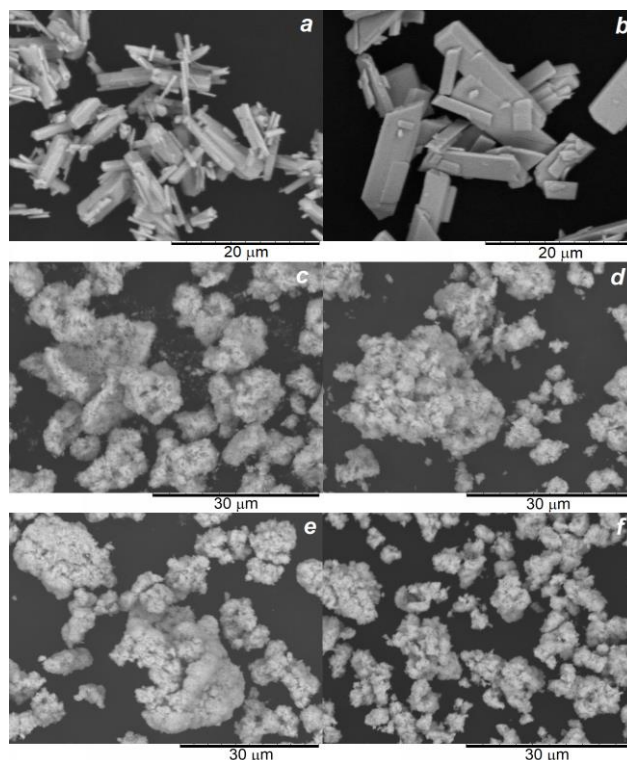
Figure 7 SEM images of the initial [Bi$_6$O$_4$(OH)$_4$](NO$_3$)$_6$·H$_2$O (a), [Bi$_6$O$_5$(OH)$_3$](NO$_3$)$_5$·3H$_2$O (b); samples DL-BiC$_4$H$_3$O$_6$ (c, d) synthesized from (a) and (b); samples β-Bi$_2$O$_3$ (e, f) obtained from (c) and (d).
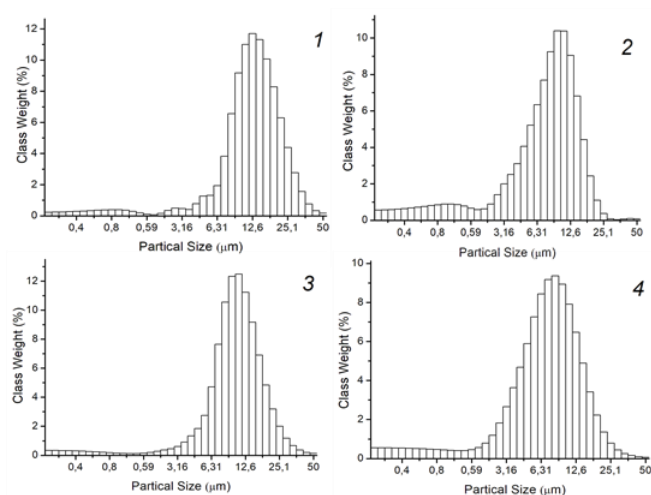
Figure 8 Grain size frequency histograms of DL-BiC$_4$H$_3$O$_6$ (1, 2) synthesized from [Bi$_6$O$_4$(OH)$_4$](NO$_3$)$_6$·H$_2$O (*1*) and [Bi$_6$O$_5$(OH)$_3$](NO$_3$)$_5$·3H$_2$O (2) and β-Bi$_2$O$_3$ (3, 4) obtained from (1) and (2) samples.

Table 1 Results of grain size analysis for samples of DL-BiC$_4$H$_3$O$_6$ and β-Bi$_2$O$_3$.

Samples	D_{50}, μm	D_I, μm	σ, μm	S_k
Precursor 1:				
DL-BiC$_4$H$_3$O$_6$ from Bi$_6$O$_4$(OH)$_4$](NO$_3$)$_6$·H$_2$O	12.0	10.67	2.24	−0.50
β-Bi$_2$O$_3$ from precursor 1	9.80	8.98	2.08	−0.41
Precursor 2:				
DL-BiC$_4$H$_3$O$_6$ from Bi$_6$O$_5$(OH)$_3$](NO$_3$)$_5$·3H$_2$O	7.78	5.93	2.62	−0.48
β-Bi$_2$O$_3$ from precursor 2	6.87	5.93	2.42	−0.41

The obtained values of the standard deviation σ are in a range of 2.00–4.00 μm, indicating a wide particle size distribution [24]. Assessment of the symmetry of the distribution curves by the degree of asymmetry ($|S_k| < 0.5$) shows that the asymmetry is insignificant for all samples [24]. The analysis of the obtained results shows that the particle size distribution in the studied samples is close to normal. This suggests that the processes of DL-BiC$_4$H$_3$O$_6$ synthesis from basic bismuth(III) nitrates occur in conditions close to equilibrium and are accompanied by recrystallization processes.

The results of grain size analysis of DL-BiC$_4$H$_3$O$_6$ and β-Bi$_2$O$_3$ powders are in agreement with the electron microscopy data and indicate smaller particle/aggregate sizes in samples synthesized using [Bi$_6$O$_5$(OH)$_3$](NO$_3$)$_5$·3H$_2$O.

4. Limitations

This work continues our previous research on the preparation of bismuth compounds with optically active and inactive isomers of oxyacids [25]. This direction in bismuth chemistry is poorly studied. At the same time, it opens up the possibility of using new synthesized compounds in engineering and medicine.

5. Conclusions

Treatment of high-purity basic bismuth(III) nitrates with DL-tartaric acid solution at molar ratio of tartrate ions to bismuth equal to 1.1 and temperature of 70 °C resulted in bismuth(III) tartrate of BiC$_4$H$_3$O$_6$ composition. It has been shown that the process of oxidative thermolysis of DL-BiC$_4$H$_3$O$_6$ includes a stage of formation of bismuth(III) oxocarbonate (BiO)$_2$CO$_3$ and metallic bismuth. After consecutive incubation of DL-BiC$_4$H$_3$O$_6$ samples in air atmosphere at 220 °C for 3–6 h and then at 280 °C for 3–6 h, fine crystalline powders of tetragonal β-Bi$_2$O$_3$, inheriting the morphology of the initial tartrates, were obtained.

● Author contributions

Conceptualization: E.V.T.
Data curation: L.I.A., E.V.T.
Formal Analysis: T.E.T., L.I.A.
Funding acquisition: E.V.T., L.I.A.
Investigation: T.E.T., E.V.T., L.I.A.
Methodology: E.V.T., L.I.A.
Project administration: E.V.T.
Resources: E.V.T., L.I.A.
Software: E.V.T., T.E.T.
Supervision: E.V.T., L.I.A.
Validation: L.I.A., T.E.T.
Visualization: E.V.T., L.I.A.
Writing – original draft: E.V.T.
Writing – review & editing: E.V.T., L.I.A.

● Conflict of interest

The authors declare no conflict of interest.

● Additional information

Author IDs:

Evgeniya V. Timakova, Scopus ID 25032239000;

Tatiana E. Timakova, Scopus ID 57929100400;

Liubov I. Afonina, Scopus ID 7006080705.

Websites:

Novosibirsk State Technical University, https://www.nstu.ru/;

Institute of Solid State Chemistry and Mechanochemistry, http://www.solid.nsc.ru/.

References

1. Amrani MA, Alrafai HA, Al-nami SY, Labhasetwar NK, Qasem A. Effect of mixing on nickel tartrate and Ni/NiO core/shell nanoparticles: Implications for morphology, magnetic, optical, dielectric and adsorption properties. Opt Mater. 2022;127:112321. doi:10.1016/j.optmat.2022.112321

2. Ye L, Duan L, Liu W, Hu Y, Ouyang Z, Yang S, Xia Z. Facile method for preparing a nano lead powder by vacuum decomposition from spent lead-acid battery paste: leaching and desulfuration in tartaric acid and sodium tartrate mixed lixivium. Hydrometal. 2020;197:105450. doi:10.1016/j.hydromet.2020.105450

3. Xu L, Jiao R, Tao X, Yi X, Wei D. One-step thermal decomposition of $C_4H_4FeO_6$ to Fe_3O_4@carbon nano-composite for high-performance lithium-ion batteries. Mater Chem Phys. 2020;239:122024. doi:10.1016/j.matchemphys.2019.122024

4. Li T, Chen J, Ma G. Self-assemble mechanism of nickel nanobelts prepared by sol-precipitation and thermal decomposition route. J Wuhan Univ Technol-Mat Sci Edit. 2022;37:206–211. doi:10.1007/s11595-022-2519-x

5. Aitlaalim A, Ouanji F, Benzaouak A, Kacimi M, Ziyad M, Liotta LF. Preparation, characterization and catalytic activity in 2-propanol conversion of potassium and antimony mixed oxides. Top Catal. 2020;63:1388–1397. doi:10.1007/s11244-020-01370-4

6. Bai X, Wang Q, Guan J. Bimetallic Iron–Cobalt Nanoparticles Coated with Amorphous Carbon for Oxygen Evolution. ACS Appl Nano Mater. 2021;4(11):12663–12671. doi:10.1021/acsanm.1c03208

7. Henaish AMA, Hemeda OM, Dorgham AM, Hamad MA. Characterization of excessive Sm^{3+} containing barium titanate prepared by tartrate precursor method. J Mater Res Technol. 2020;9(6):15214–15221. doi:10.1016/j.jmrt.2020.10.015

8. Nighot DV, Khanvilkar MB, Karale NJ, Pawar RA, Gugale GS, Arbuj SS, Nikumbh AK. Investigation on solid state pyrolytic decomposition of bimetallic fumarate and tartrate precursors of Co(II), Ni(II) and Zn(II) with manganese. Mater Today Proc. 2022;49:1351–1359. doi:10.1016/j.matpr.2021.07.057

9. Ahadiat G, Tabatabaee M, Gholivand K, Zare K, Dusek M, Kucerakova M. A two-dimensional bismuth coordination polymer with tartaric acid: synthesis, characterization and thermal decomposition to Bi_2O_3 nanoparticles. Main Group Chem. 2017;16:7–16. doi:10.3233/mgc-160216

10. Morandi P, Flaud V, Tingry S, Cornu D, Holade Y. Tartaric acid regulated the advanced synthesis of bismuth-based materials with tunable performance towards the electro-catalytic production of hydrogen peroxide. J Mater Chem A. 2020;8:18840–18855. doi:10.1039/d0ta06466a

11. Diktanaite A, Gaidamaviciene G, Kazakevicius E, Kezionis A, Zalga A. Aqueous sol-gel synthesis, thermal analysis, characterization and electrical properties of V_2O_5 doped Bi_2O_3 system. Thermochim Acta. 2020;685:178511. doi:10.1016/j.tca.2020.178511

12. Afonina LI, Timakova TE, Timakova EV, Gerasimov KB, Yukhin YM. Thermal transformations of bismuth(III) tartrates. Chimica Techno Acta. 2022;9(3): 20229315. doi:10.15826/chimtech.2022.9.3.15

13. Daminov AS, Yukhin YM, Naydenko ES. Processing of Nitrate Solutions for the Preparation of Basic Bismuth Nitrate and Oxide. Theor Found Chem Eng. 2020;54:1020–1025. doi:10.1134/s0040579520050097

14. Yukhin YM, Mishchenko KV, Daminov AS. Bismuth preoxidation for preparing solutions of salts. Theor Found Chem Eng. 2017;51:495–502. doi:10.1134/s0040579517040303

15. Fukami T, Tahara S, Dimyati A. Crystal Structures and Thermal Properties of L-$MnC_4H_4O_6 \cdot 2H_2O$ and DL-$MnC_4H_4O_6 \cdot 2H_2O$. Inter J Chem. 2020;12(1):78–88. doi:10.5539/ijc.v12n1p78

16. Fukami T, Tahara S. Structural and thermal investigations of L-$CuC_4H_4O_6 \cdot 3H_2O$ and DL-$CuC_4H_4O_6 \cdot 2H_2O$ single crystals. Inter J Chem. 2021;13(1):38–49. doi:10.5539/ijc.v13n1p38

17. Zhang X, Yue J, Zhao Y, Yan Z, Zhu G, Liu L, Xu H, Yu A. Synthesis of tetragonal $BaTiO_3$ nano-particle via a novel tartaric acid co-precipitation process. Ceram Int. 2021;47(5):7263–7267. doi:10.1016/j.ceramint.2020.11.006

18. Sasikala V, Sajan D, Vijayan N, Chaitanya K, Babu Raj MS, Selin Joy BH. Growth, molecular structure, NBO analysis and vibrational spectral analysis of l-tartaric acid single crystal. Spectrochim Acta Part A. 2014;123:127–141. doi:10.1016/j.saa.2013.12.045

19. Vidya S, Ravikumar C, Hubert Joe I, Kumaradhas P, Devipriya B, Raju K. Vibrational spectra and structural studies of nonlinear optical crystal ammonium D,L-tartrate: a density functional theoretical approach. J Raman Spectrosc. 2011;42:676–684. doi:10.1002/jrs.2743

20. Bhattacharjee R, Jain YS, Raghubanshi G, Bist HD. Laser Raman and infrared spectra of Rochelle salt crystals. J Raman Spectrosc. 1988;9(1):51–58. doi:10.1002/jrs.1250190108

21. Xiao J, Zhang H, Xia Y, Li Z, Huang W. Rapid and high-capacity adsorption of sulfonated anionic dyes onto basic bismuth(III) nitrate via bidentate bridging and electrostatic attracting interactions. RSC Adv. 2016;6:39861–39869. doi:10.1039/c6ra03055f

22. Nakamoto K. Infrared and Raman Spectra of Inorganic and Coordination Compounds. Part B: Application in Coordination, Organometallic and Bioinorganic Chemistry. 6th Edition. New Jersey: Wiley & Sons; 2009. 57–61 p.

23. Klinkova LA, Nicolaichik VI, Barkovskii NV, Fedotov VK. Thermal stability of Bi_2O_3. Russ J Inorg Chem. 2007;52:1822–1829. doi:10.1134/S0036023607120030

24. Blott SJ, Pye K. GRADISTAT: a grain size distribution and statistics package for the analysis of unconsolidated sediments. Earth Surf Process Landforms. 2001;26:1237–1248. doi:10.1002/esp.261

25. Timakova EV, Afonina LI, Yukhin YI, Bulina NV, Volodin VA. Preparation of Bismuth(III) Malates by Precipitation from Nitrate Solutions. Chem Sustain Dev. 2017;25(3):293–300. Available from: https://sibran.ru/upload/iblock/3a2/preparation_of_bismuth_iii_malates_by_precipitation_from_nitrate_solutions.pdf. Accessed on 28 June 2023